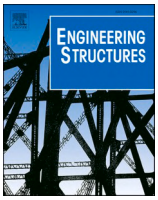
Engineering Structures 245 (2021) 112892



Contents lists available at ScienceDirect

Engineering Structures

journal homepage: www.elsevier.com/locate/engstruct





Retrofitting of shear-damaged RC T-beams using U-shaped SHCC jacket

Ali Hassan *, Ahmed T. Baraghith, Ahmed M. Atta, Tarek F. El-Shafiey

Department of Structural Engineering, Tanta University, Tanta, Egypt

ARTICLE INFO

Keyword:
Shear
Cracked
Beams
Repairing
Strengthening
Strain-hardening cementitious composite (SHCC)
Concrete

ABSTRACT

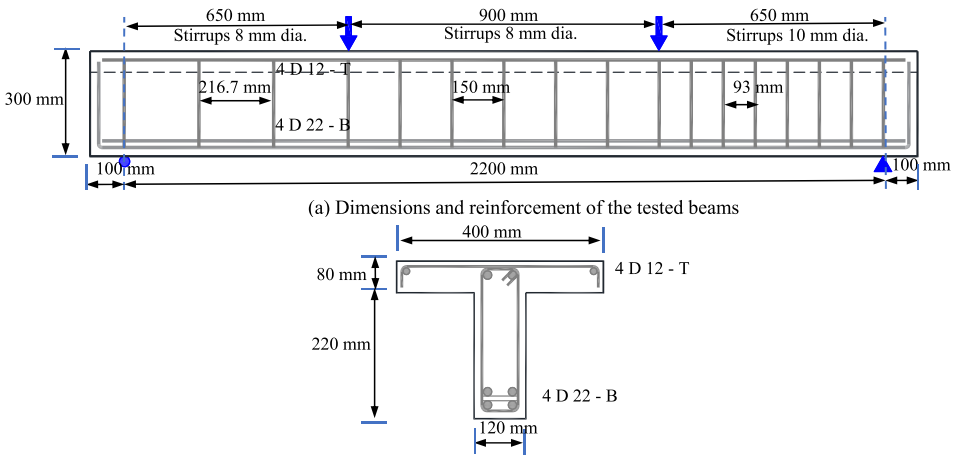
Strengthening of Reinforced Concrete (RC) beams using Strain-Hardening Cementitious Composites (SHCC) material became a worldwide practice. Previous investigations showed significant improvement in the shear resistance of SHCC-strengthened (undamaged) beams. However, a little effort has been devoted to study the ability of SHCC material in retrofitting shear-damaged RC beams. Thus, the current study aims to evaluate the shear response of shear-damaged RC beams repaired with SHCC material. In this context, eleven RC beams were prepared and configured to be failed in shear. One beam was considered as control specimen; while, four beams were strengthened with 20 mm thick U-shaped SHCC jackets having four different transversal reinforcement ratios (0, 0.65, 0.86 and 1.08%). The remaining six beams were pre-cracked (preloaded) with three different preloading levels (0.75, 0.85 and 0.95% of the ultimate capacity), then, three differently preloaded beams were repaired with SHCC jackets, whereas, for the remaining three beams, the developed shear cracks were injected by epoxy prior to the application of SHCC jackets. All beams were tested under four point loading scheme with shear span-to-depth ratio of 2.5. The test results showed that the strength, post-peak deformability and shear-crack response of the repaired beams were improved compared to those of the control beams. In addition, the use of epoxy injection prior to the application of the SHCC jacket showed its ability to restore a significant value of the lost strength gain due to preloading. However, the repairing technique was not able to restore the initial stiffness of the uncracked beams. Finally, based on analytical analysis, the design equations of JSCE code underestimated the ultimate shear capacity of the strengthened/repaired beams with average safety margin of about 27%.

1. Introduction

Retrofitting of RC beams may be needed due to various reasons. Many techniques can be used for upgrading the shear strength of the RC defected beams. In the last two decades, many experimental and theoretical investigations have been performed to evaluate the shear behaviour of RC beams strengthened with Fiber Reinforced Polymer (FRP) sheets [1–10]. FRP has many advantages such as high strength to weight ratio, good durability coupled with a very adequate implementation strategy for many RC structures [10]. However the above advantages, there are many disadvantages sometimes obstruct the use of externally bonded FRP sheets. The FRP has a low fire resistance and thus following expensive fire protection cost [10]. In addition, in case of cracked beams, the existence of cracks may affect the composite action between the FRP sheets and the substrate concrete, thus, the FRP is not recommend to be applied to a cracked concrete surface [11]. To overcome some of the drawbacks associated with FRP composites, a new composite material namely Fabric-Reinforced Cementitious Matrix (FRCM) has been developed as an alternative to eternally bonded FRP by replacing of epoxy adhesive material by cementitious matrix. Owing to the use cementitious matrix instead of epoxy, FRCM inherently possesses much better fire resistance compared to FRP. Moreover, FRCM experienced better compatibility with the substrate concrete under moist environments [12,13]. To date, numerous experimental investigations were carried out to investigate the effectiveness of FRCM systems for restoring the shear strength of deficient RC beams [14,15]. Another shear strengthening technique is to bond steel plates to the vertical surfaces of RC beams in order to increase their strength [16,17]. The steel plates may be bonded or bolted [18–21] on the vertical surfaces of the RC beam. This strengthening technique showed a better ductility as well as enhanced failure mode in comparison with the FRP sheets [22–25]. Nevertheless, this technique may weaken the RC beam after drilling of bolts' holes and the external steel plates are susceptible to corrosion [20].

* Corresponding author at: Structural Engineering Dept. Faculty of Engineering, Tanta University, Tanta 31511, Egypt.
E-mail address: ali_hassan@f-eng.tanta.edu.eg (A. Hassan).

https://doi.org/10.1016/j.engstruct.2021.112892
Received 2 December 2020; Received in revised form 7 July 2021; Accepted 21 July 2021
Available online 29 July 2021
0141-0296/© 2021 Elsevier Ltd. All rights reserved.



(a) Dimensions and reinforcement of the tested beams

(a) Cross-section of the tested beams

Fig. 1. Details of the tested beams.

Strain Hardening Cementitious Composites (SHCC) is a newly developed cement based morter reinforced with short fibers around a volume fraction of 2%. SHCC showed a steady state of multiple cracking and strain-hardening response under tensile stresses prior to cracks localization [26–30]. High strength and high modulus polymeric fibers are used in the development of SHCC [25]. Generally, the tensile strain hardening phenomena of SHCC is obtained by tailoring the cementitious paste using randomly oriented short fibers following micromechanics based theory [31–33]. The superior tensile strain-hardening property of SHCC gave it the priority to be used in many structural applications where the issues pertaining to crack control, ductility and energy absorption are dominant [34].

In case of external shear/flexural strengthening, the shear transformation between the substrate concrete and the strengthening material is considered as a critical issue [35]. Xue and Deng [36] compared the bond behavior of SHCC/concrete and concrete/concrete interface, and concluded that, the interaction between SHCC/concrete was better than that of concrete/concrete. Wang [37] examined the slant shear performance of SHCC/concrete interface. The experiments showed that the bond strength of SHCC/concrete increased with increasing the interface roughness. In addition, increasing the substrate concrete strength significantly improved the interface bond strength. Slowik et al. [38] suggested that it is possible to achieve the balance between the interface debonding and SHCC cracking by varying the interface roughness and bond strength. Kim et al. [39] examined the interfacial bond performance of a sprayed SHCC for repair applications. Kim concluded that, sufficient interfacial bond performance and enhanced energy absorption capacity of the SHCC repair system were obtained.

An original driving force behind the development of SHCC was the possible improvement of structural safety given the failure of some RC structures. Since then, extensive investigations at the structural element level have showed a great enhancement in the structural resilience characterized by delayed collapse and rapid recovery of structural functions post-events [40–46]. These experimental investigations were conducted for columns, beams, beam-column connections, walls, and frames. In the field of shear strengthening applications, Kim et al. [47] studied the shear behaviour of RC beams strengthened with SHCC. The experimental investigation showed that the use of SHCC layer increased the shear capacity as well as the ductility of the tested beams. Furthermore, SHCC layer was found to be effective for enhancing the cracking behaviour. Wang et al. [48] studied the shear behaviour of RC beams strengthened with SHCC material. A layer of 20 mm thick of SHCC was sprayed onto the sides of the tested beams. Wang et al. concluded that, the ultimate shear load of the tested beams increased by 89% over than the benchmark unstrengthened beam. Baghi et al. [49] examined the potentialities of precast SHCC plates as a shear strengthening technique for RC beams. As per Baghi observations, the use of SHCC plates was capable of arresting the crack propagation and increasing the ultimate capacity. Zheng et al. [50] carried-out an experimental and numerical investigation to evaluate the shear performance of RC beams strengthened with FRP-SHCC composite layer. According to Zheng, a good bond between the FRP-SHCC and the substrate concrete was exhibited. In addition, a great improvement in the shear capacity of the strengthened beams was achieved. Yang et al. [51] studied the shear performance of FRP grid-reinforced SHCC matrix. Based on the experimental findings, the gained shear strength of the strengthened beams ranged between 50.9% and 160.6% in comparison with the unstrengthened beam. Shang et al. [52] examined the response of fire-damaged RC beams shear retrofitted by stirrup of SHCC material. It was found that the SHCC is an adequate strengthening technique for fire damaged RC beams [52]. Hassan et al. [53] studied the shear behaviour of RC beams with web openings strengthened with precast SHCC plates. According to Hassan et al. recommendations, the use of SHCC material enabled the strengthened beams to demonstrate a distinguished performance in terms of ultimate load and ductility.

As presented in the above section, most of the previous investigations were performed to study the structural performance of RC beams strengthened with SHCC material. However, many problems are still in need to be studied. For instance, most of structural elements, which are needed to be retrofitted are in damage state; however, most of the previous investigations were carried out on beams strengthened without being initially damaged. Therefore, it is important to investigate the shear response of initially damaged RC beams shear-repaired with SHCC jackets. In addition, for such pre-damaged repaired beams, the accuracy of the current shear capacity prediction models are also in need to be evaluated.

The present work is devoted to investigate the following targets; (1) the structural performance of shear-damaged RC beams repaired with SHCC jackets, (2) the enhancement in the shear response induced by suppressing the shear cracks at the damaged zone by epoxy injection prior to the application of SHCC jackets, (3) the accuracy of the design equations of JSCE code to predict the shear capacity of repaired beams. In accordance with these targets, eleven RC T-beams were prefabricated. One reference beam was tested without strengthening. Whereas, four of these beams were strengthened using U-shaped SHCC jackets having four different transversal reinforcement ratios (0, 0.65, 0.86 and 1.08%). The remaining six beams were firstly preloaded by three different preloading levels; 75, 85, and 95% of the ultimate capacity. Afterwards, these beams were repaired using two different techniques. The first technique was the application of SHCC jacket without any

Table 1
Test parameters.

Group No.	Beam ID	Preloading level, % of P_u for BC	Strengthening regime	Epoxy injection	Jacket's stirrups		Jacket's reinforcement ratio, %	Objectives
					Diameter, mm	Spacing, mm		
Control	BC	0	–	–	–	–	–	reference
Group I	$B_{0\text{-}SJ\text{-}0}$	0	SJ	–	–	–	–	Studying the effect of jacket's reinforcement ratio
	$B_{0\text{-}RSJ\text{-}0.65}$	0	RSJ	–	6	216.7	0.65	
	$B_{0\text{-}RSJ\text{-}0.86}$	0	RSJ	–	6	162.5	0.86	
	$B_{0\text{-}RSJ\text{-}1.08}$	0	RSJ	–	6	130.0	1.08	
Group II	$B_{1\text{-}RSJ\text{-}1.08}$	75	RSJ	–	6	130.0	1.08	Studying the effect of preloading level
	$B_{2\text{-}RSJ\text{-}1.08}$	85	RSJ	–	6	130.0	1.08	
	$B_{3\text{-}RSJ\text{-}1.08}$	95	RSJ	–	6	130.0	1.08	
Group III	$B_{1\text{-}IRSJ\text{-}1.08}$	75	IRSJ	Injected	6	130.0	1.08	Studying the effect of epoxy injection
	$B_{2\text{-}IRSJ\text{-}1.08}$	85	IRSJ	Injected	6	130.0	1.08	
	$B_{3\text{-}IRSJ\text{-}1.08}$	95	IRSJ	Injected	6	130.0	1.08	

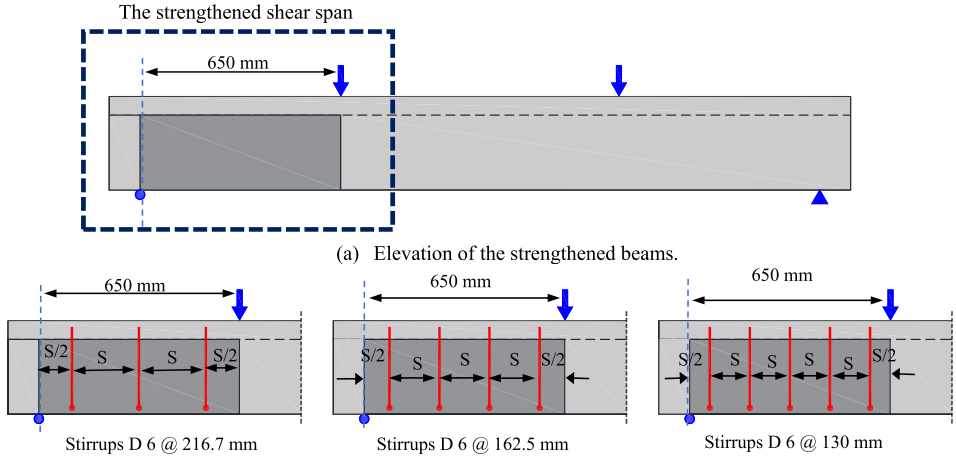
P_u = ultimate load; *SJ* = SHCC Jacket; *RSJ* = Reinforced SHCC Jacket; *IRSJ* = Epoxy injection prior to the application of RSJ.

treatment to the cracks, which developed during the preloading stage. While, the second technique was to inject the cracks by epoxy adhesive prior to the application of SHCC jacket. The test program outputs in forms of cracking loads, ultimate loads, deformational characteristics and shear-crack width development were presented. Eventually, the existing shear prediction models of JSCE-code were verified with the obtained experimental results.

2. Experimental work program

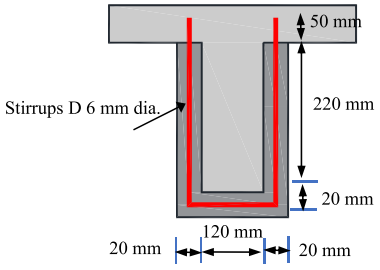
2.1. Test program

In the current experimental investigation, eleven reduced scale RC T-beams with 2400 mm total length were prefabricated. As shown in Fig. 1, the beam's top flange was 400 mm width and 80 mm thickness.



(a) Elevation of the strengthened beams.

(b) Distribution of the stirrups in the strengthened shear span for the reinforced jackets



(c) Cross-section of the strengthened beams at jacketed part

Fig. 2. Details of the strengthened beams.

Table 2
Mix ingredients of the used materials (kg/m^3) for cubic meter.

W/B	Water	Super plasticizers	Fiber (Volumetric ratio %)	Coarse aggregate	Sand	Silica fume	Cement	Material
0.5	175	–	–	1279	535	–	350	NSC
0.20	312.1	31.6	16.20 (2.0%)	–	157.9	237	1342	SHCC

NSC = Normal strength concrete; *SHCC* = Strain-Hardening Cementitious Composites; *W/B* = water-to-binder ratio.

Where, the beam's web was 120 mm width and 300 mm total height. The beam had an effective depth (d) of 260 mm and the effective shear span (a) was 650 mm. Accordingly, the shear-span to depth ratio (a/d) was 2.5 (the minimum ratio to avoid the arch action [54]). To assure shear failure, the beams were intensively reinforced with high strength steel in flexure. The longitudinal reinforcement consisted of 4 D 22-B (D = diameter and B = bottom) and 4 D 12-T (T = top). With regard to the transverse reinforcement, normal mild steel stirrups with 8 mm diameter every 216.7 mm (spacing) were used in the studied shear span. Whereas, to prevent shear failure in the other shear span, high strength steel stirrups with 10 mm diameter every 93 mm (spacing) were used. Table 1 summarizes the details of the tested beams. As shown in Table 1, the first group of this study consists of four strengthened beams (i.e. uncracked beams), which were strengthened using U-shaped SHCC jacket with 20 mm thickness (t_{SHCC}). The studied parameter of group I was the jacket's transversal reinforcement ratio (μ), four ratios were studied; 0, 0.65, 0.86 and 1.08%. The transversal jacket's reinforcement ratio (μ) was obtained by Eq. (1). Previous investigations demonstrated that the transversal reinforcement is one of the governing parameters that affects the shear capacity along with the width of the developed shear cracks [55,56]. In addition, it was found that, for the same amount of reinforcement, increasing the stirrups number with decreasing its diameter lead to a better cracking behaviour by precluding the early localized crack [57]. Accordingly, normal mild steel stirrups with 6 mm diameter (bar's cross-sectional area (A_{bar}) = 28.26 mm^2) were used. For the jackets transversal reinforcement ratios of 0.65, 0.86 and 1.08% the stirrups spacing (S) were 216.7, 162.5 and 130 mm, respectively. The details of the used jacket's transversal reinforcement are depicted in Fig. 2.

$$\mu = \frac{A_{bar}}{t_{SHCC}.S} \tag{1}$$

where; μ = web reinforcement ratio; A_{bar} = cross-sectional area of the used bar; t_{SHCC} = thickness of SHCC jacket; S = horizontal spacing between stirrups.

On the other hand, to evaluate the ability of the proposed repairing technique to restore the shear strength of pre-cracked RC beams, six of the prefabricated beams were firstly preloaded to three different levels of damage. These levels of preloading were selected based on the ultimate capacity of the control unstrengthened beam (180 kN). The preloading levels were 75, 85, and 95% of the ultimate load (P_u) (i.e. the preloads were 135, 153 and 171 kN). After the completion of the preloading stage, the preloaded beams were repaired with two different repairing techniques. Group II consisted of three differently preloaded beams, which were repaired using SHCC jackets. On the other hand, group III consisted of three beams similar to group II, while the beams' shear cracks were injected with epoxy adhesive material prior to the application of SHCC jackets. It worth mentioning that, for all beams of groups II and III, the SHCC jacket's thickness was 20 mm and the jacket's reinforcement ratio was 1.08%.

2.2. Beam's designation

As shown in Table 1, the reference unstrengthened beam was symbolized by the capital letters BC. Whereas, the remaining retrofitted beams were designated by the letter B followed by three subscript symbols. The first symbol indicates the preloading level reached prior to the application of the repairing technique (1 = 75% of P_u, 2 = 85% of P_u and 3 = 95% of P_u). Where, the second symbol depicts the used repairing procedure (SJ = plain SHCC jacket, RSJ = Reinforced SHCC jacket and IRSJ = Injection of the developed shear cracks with epoxy adhesive prior to casting of the SHCC jacket). Finally, the last symbol refers to the jacket's reinforcement ratio (0 = unreinforced jacket; 0.65, 0.86 and 1.08 = percentage of jacket's transversal reinforcement ratio (%)).

Table 3
Characteristics of the used steel reinforcement.

Modulus of elasticity, GPa	Ultimate strength, MPa	Yield strength, MPa	Diameter, mm
205	352	242	6
205	360	240	8
205	602	400	10
205	605	402	12
205	610	405	22

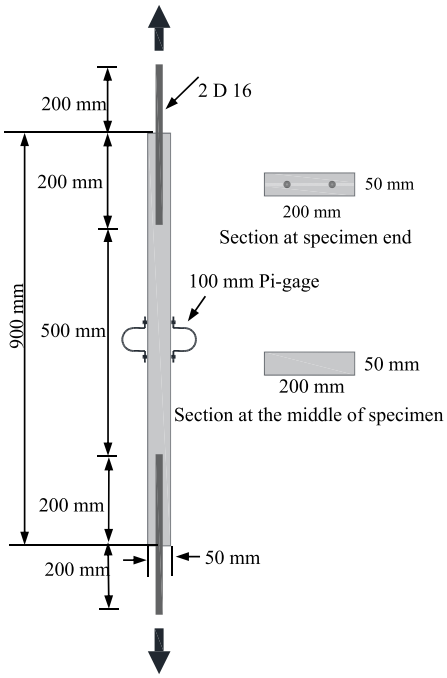
2.3. Material properties

To avoid the variation in concrete strength of the tested beams, the same patch of a ready-mixed concrete was used in all beams. Table 2 summarizes the used concrete mix ingredients for cubic meter (kg/m^3). Ordinary Portland cement (Type I) and water-to-cement (w/c) ratio of 0.50 was used in this mix. The used fine aggregates were a cleaned river sand with density of 2650 kg/m^3. Whereas the used coarse aggregates were a limestone with a nominal maximum size of 20 mm and a density of 2700 kg/m^3. At the test date of the beams, compression tests were carried out on standard cylinders with 300 mm height and 150 mm diameter as per ASTM C39/C39M. At the test date, the mean cylinder compressive strength ($f_c^{'}$) was 35.2 MPa. Additionally, Brazilian tensile tests were carried-out on three cylinders to obtain the actual tensile strength. The mean tensile strength at the test date was 3.40 MPa.

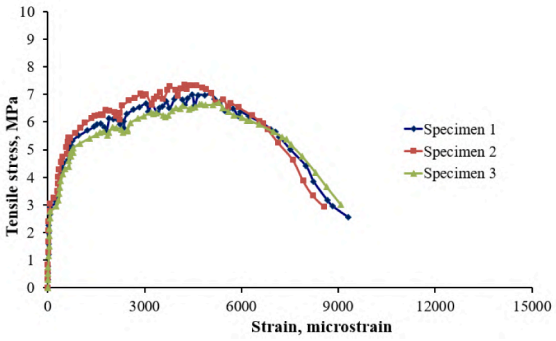
Two grades of steel reinforcement were used in the tested beams: grade 240/350 (N.M.S) plain round bars with diameters of 6 and 8 mm; grade 400/600 (H.T.S) ribbed bars with nominal diameters of 10, 12 and 22 mm. For each diameter, tensile tests were carried out on three standard specimens. Table 3 reports the mean values yield and ultimate strengths as well as the average modulus of elasticity for the tested specimens.

The ingredients of the used SHCC mix for cubic meter (kg/m^3) are reported in Table 2. The SHCC mix consisted of; Ordinary Portland cement, fine silica sand with the gain size below 0.32 mm, silica fume with average diameter between 0.1 μm and 0.3 μm, polypropylene (PP) fibers, water and superplasticizers. As reported in the manufacture's datasheet, the PP fibers had a length of 12 mm and diameter of 25 μm. The PP fibers had a maximum tensile strength of 2900 MPa, a maximum fiber's elongation of 2.42%, and a modulus elasticity of 116 GPa. In this study, the volume fraction of fibers in the mix was 2%.

During the repairing stage, samples from the SHCC mix were prepared to figure out the tensile and compressive characteristics. To avoid the size effect on the ultimate tensile strain of SHCC material, Li et al. [28] and Kunieda et al. [58] recommended performing the uniaxial tensile tests on large size specimens. The recommended size has a cross-section of 50 × 200 mm and a length of 900 mm. As per the recommendations of [28,58] the direct uniaxial tensile tests were carried out on three specimens. The specimens were loaded with a displacement-controlled system with a loading rate of 0.005 mm/s. Fig. 3a shows



(a) Dimensions of the axial tension test specimens



(b) Stress-strain relationship of SHCC material under uniaxial tension

Fig.3. Specimen's dimensions and stress–strain curves of axial tension tests.



(a) Preloaded by 75% of ultimate load for BC

(b) Preloaded by 85% of ultimate load for BC

(a) Preloaded by 95% of ultimate load for BC

Fig. 4. Samples of the precracked beams with different levels of damage.

the dimensions of the axial tension test specimen and Fig. 3b shows the obtained tensile stress–strain curves of the tested SHCC specimens. As shown in Fig. 3b, the mean first-cracking strength of the used SHCC was 3.13 MPa, while, the mean ultimate tensile strength was 7.14 MPa. Furthermore, the compressive tests were carried-out on three cylinders. The specimen was 100 mm height and 50 mm diameter. The average compressive strength of the tested specimens was about 65.54 MPa.

One of the governing parameters in the repairing process is the bond between the substrate concrete and the repairing material. As per ASTM C882-99, the slant shear tests were performed on three cylindrical specimens. The first half of the cylinder was cast with the concrete mix that used in the tested beams. After 28 days, the contact surface was roughened using mattock (roughening depth was 5 mm). Thereafter, the SHCC material was applied to the substrate concrete, which was in a water-saturated surface condition. After 28 days, the specimens were tested under a compression test scheme. The splitting failure took-place at the direction of loading without sliding and the mean value of the slant shear strength was 17.90 MPa.

A structural resin epoxy (Kemapoxy 103) was used to fill the developed cracks of the preloaded beams of group III. As per the manufacturer's specifications, the used epoxy density is 1.10 ± 0.02 kg/L and its initial and final setting times are 8 and 24 h, respectively. Whereas, the complete hardening of the used epoxy takes place after 7 days.

2.4. *Repair/strengthening process*

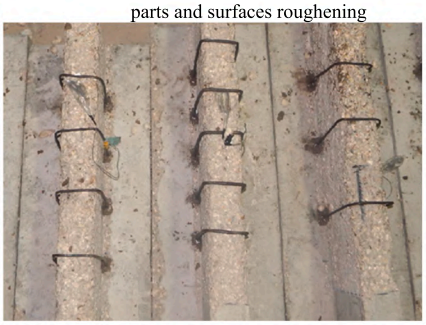
As listed in Table 1, the beams of groups II and III were preloaded by three different preloading levels: 75, 85 and 95% of the ultimate load of beam BC (the ultimate load was 180 kN). Fig. 4 shows three beams of the preloaded beams after reaching the target pre-damage levels. The retrofitting of the pre-damaged beams of groups II and III includes the following steps: (1) As shown in Fig. 5a, in the studied shear span, the surfaces of each beam were roughened using mattock (the roughening depth was around 5 mm). (2) The cracks were cleaned from dust and debris using an air blower. (3) The cracks' surfaces were widened to approximately 5 mm. (4) After fixing injection pipes, the beam's surfaces were sealed using a quick setting mortar to prevent the epoxy leakage during the injection stage, as shown in Fig. 5b. (5) The shear cracks were injected with a structural resin epoxy using a high-pressure pump. (6) The designed U-shaped stirrups were planted in the critical shear span using adhesive mortar, as shown in Fig. 5c. (7) After 24 h, the SHCC jacket was cast using a wooden shuttering, as shown in Fig. 5d. It worth mentioning that, the repairing procedure of group II included only the steps; 1, 2, 6 and 7 (i.e. repaired without epoxy injection).



(a) Image of a test beam after removing of the weak parts and surfaces roughening



(b) Image of a test beam after covering the cracked part with quick setting mortar



(c) Image of test beams after planting the designed U-shaped stirrups



(d) Image of test beams after casting of the SHCC jackets

Fig. 5. Images during the repairing steps of the test beams.

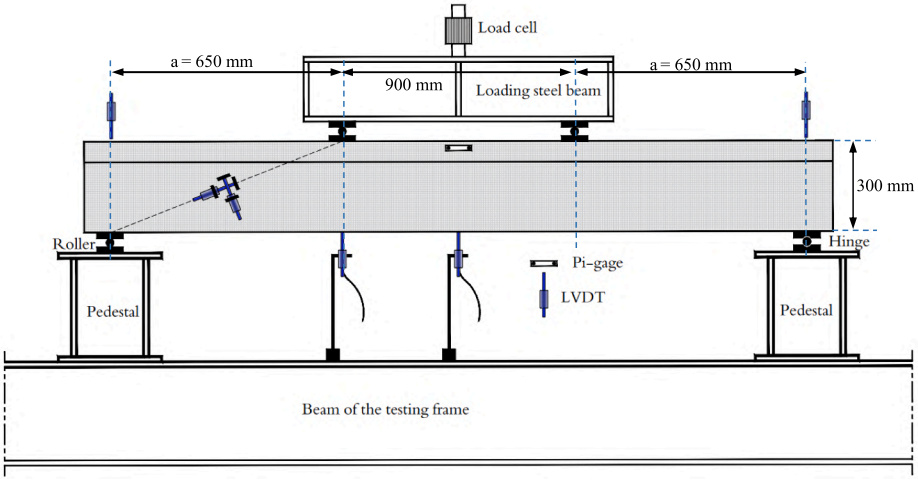


Fig. 6. Test setup and instrumentations.

2.5. Loading and test scheme

As shown in Fig. 6, all beams were tested under a four-point bending test. The beams span from support to support was 2200 mm, and the shear-span-to-effective depth ratio was 2.5, which is considered the minimum ratio to neglect the arch action effect [54]. Under a monotonic load-controlled scheme, all beams were loaded with a rate of 5 kN/min. The load was monitored using a load cell with maximum capacity of 500 kN. Two LVDTs (100 mm gauge length) were used to record the developed deflection one at mid span and another under the loading point. In addition, two LVDTs were positioned over the two supports. In the studied shear span, two LVDTs (45°-rosette) were placed on the middle of the line connecting the load with the support to measure the developed shear strain. Strain gauges (5 mm gauge length) were bonded to the stirrups in the critical shear span and longitudinal tension steel reinforcement. In addition, in case of U-stirrups were used in the SHCC jackets, strain gauges were bonded to the stirrups prior to casting of the SHCC. One Pi-gauge displacement transducers (100 mm gauge length and 0.005 accuracy) was used to record the compressive strain of concrete. After each loading interval, an optical microscope (0.01 mm accuracy) was used to measure the major crack width in flexure and shear. For all tests, an automatic data acquisition system was used to collect the test data from the load cell, Pi-gauge, LVDTs, and the strain gauges.

3. Experimental results

3.1. Ultimate load and failure modes

The cracking patterns at failure of all beams are shown in Fig. 7. For the reference unstrengthened beam (BC), the first visible flexural crack occurred within the loading zone when the load reached about 90 kN. Increasing the applied load, the first shear crack took-place in the studied shear span at about 96 kN. With further increase in the applied load, the major shear crack growth and widened. At about 180 kN, the

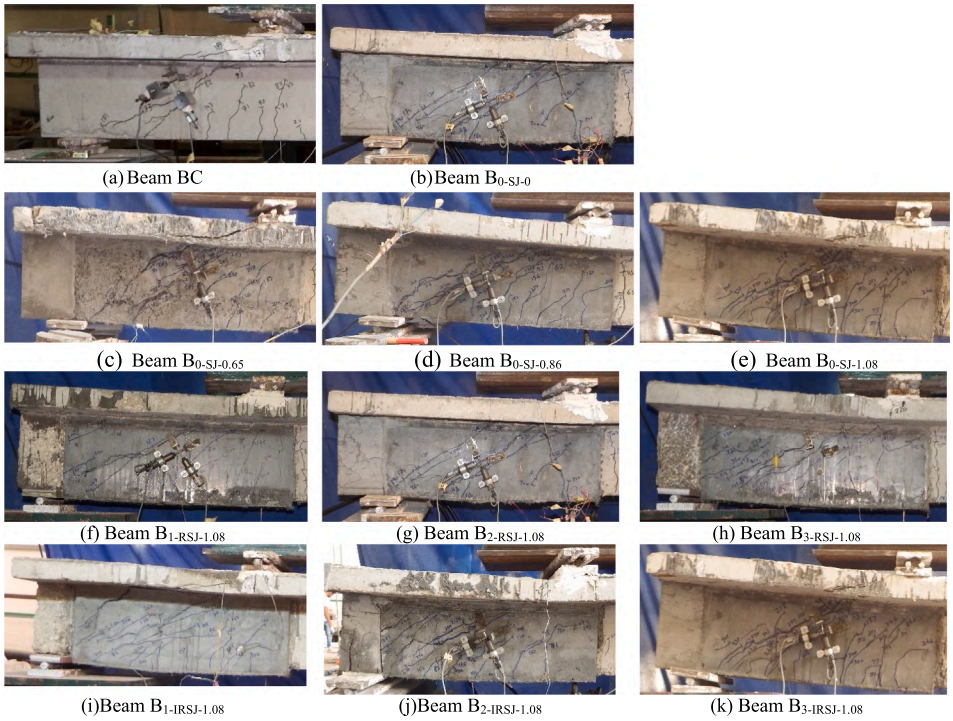


Fig. 7. Failure modes of the tested beams.

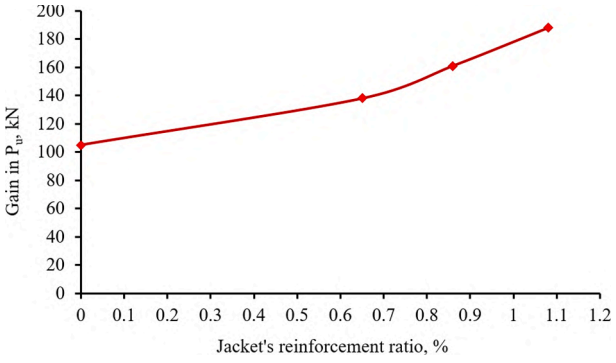


Fig. 8. Gain in P_u vs. jacket's reinforcement ratio.

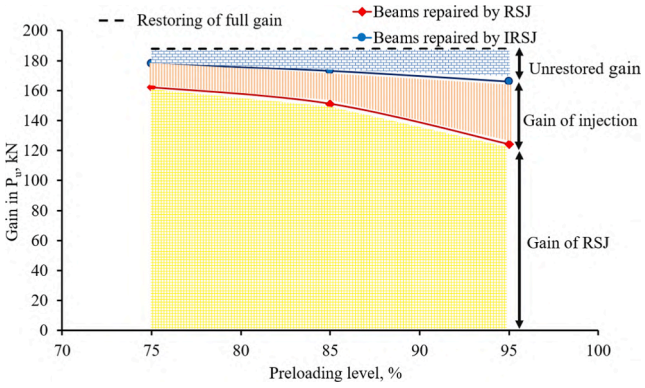


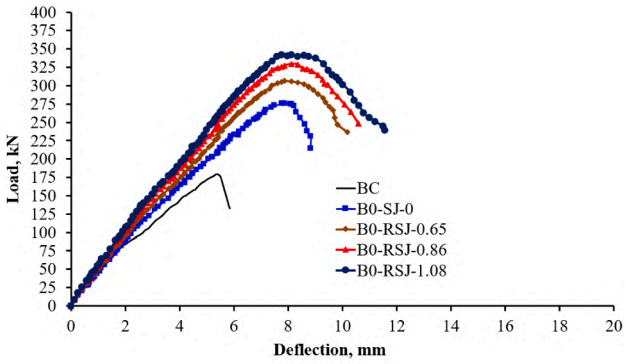
Fig. 9. Gain in Pu vs. preloading level.

shearing failure suddenly occurred. Checking the failure cracking pattern of beam BC presented in Fig. 7a, almost a single shear crack on the direction of the line connecting support and loading points was noticed.

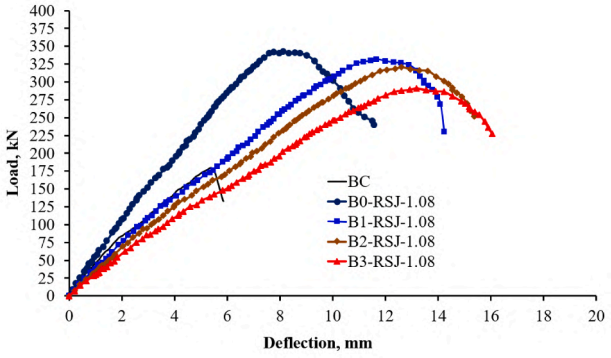
Group I was tested to evaluate the effect of the jacket's reinforcement ratio on the shear response, therefore, four different jacket's reinforcement ratios were investigated (μ = 0, 0.65, 0.86, 1.08%). Comparing the cracking pattern of group I, the use of the SHCC jacket did not alter the failure mode of the strengthened beams, as shown in Fig. 7b–e. All beams of group I failed in shear manner with a clear rupture of SHCC jackets along the shear cracks. Whereas, compared to the unstrengthened beam (BC), the effect of fibers bridging action of the SHCC material was clear, thus, more shear cracks developed with the use of SHCC jacket. Furthermore, the number of the developed cracks increased with the increase of jacket's reinforcement ratio, causing a fine multi-able shear cracks.

Fig. 8 plots the relation between the jacket's reinforcement ratio vs. the gain in ultimate capacity in kN. As shown in Fig. 8, the effect of jacket's reinforcement ratio was clear, with the increase of the reinforcement ratio, the obtained gain increased. For this reason, beam $B_{0\text{-}RSJ\text{-}1.08}$ recorded the highest strength gain in comparison with the similar beams. The ultimate capacity of $B_{0\text{-}RSJ\text{-}1.08}$ was 368 kN (104% and 28% higher than those of beams BC and $B_{0\text{-}RSJ\text{-}0}$, respectively).

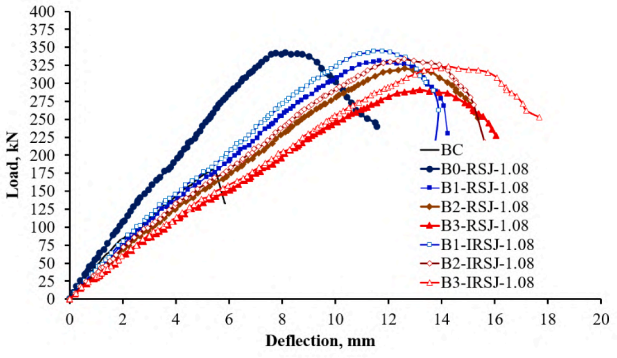
To evaluate the influence of pre-cracking degree on the efficiency of the proposed technique, group II was tested. In this group, beams $B_{1\text{-}RSJ\text{-}1.08}$, $B_{2\text{-}RSJ\text{-}1.08}$ and $B_{3\text{-}RSJ\text{-}1.08}$ were initially loaded to three different preloading levels 75, 85 and 95% of the ultimate load, thereafter, these beams were strengthened with SHCC jackets. Comparing the obtained results of group II with the similar uncracked beam $B_{0\text{-}RSJ\text{-}1.08}$, the pre-cracked beams of group II exhibited similar crack patterns owing to identical SHCC characteristics, however, the ultimate load was relative to the level of damage. Fig. 9 shows the relationship between the preloading level and the obtained strength gain. As shown in Fig. 9, there is an inverse relationship between the strength gain and the preloading level, as the preloading level increased the obtained strength gain seriously decreased. For instance, the achieved gain of beam $B_{3\text{-}RSJ\text{-}1.08}$ (95% preloading level) was 124 kN, which represent about 65.9% of that achieved by beam $B_{0\text{-}RSJ\text{-}1.08}$ (strengthened without preloading). This may be attributed to the decrease of aggregate interlock mechanism in pre-cracked beams which reduced the shear strength shared by concrete, this result is consistent with previous researchers [11,59].



(a) Curves of BC and group I



(b) Curves of BC, $B_{0\text{-RSJ-}0.72}$, group II



(c) Curves of BC, $B_{0\text{-RSJ-}0.72}$, group II and group III

Fig. 10. Load-deflection curves for the tested beams.

To evaluate the impact of the epoxy injection, beams $B_{1\text{-IRSJ-}1.08}$, $B_{2\text{-IRSJ-}1.08}$ and $B_{3\text{-IRSJ-}1.08}$ were tested. For these beams, the cracks developed during the preloading stage were injected with epoxy prior to the application of SHCC jackets. Comparing the test results of this group with group II, the beams of group III failed in shear with a similar cracking pattern obtained by group II, as shown in Fig. 7i–k. Based on the achieved strength gains, interesting results were observed, when the preloading level was 75%, the conjunction of epoxy injection with SHCC jacket was able to achieve strength capacity near to that obtained by the uncracked beam. The ultimate capacity of beam $B_{1\text{-IRSJ-}1.08}$ was 358 kN, about 97% of that achieved by beam $B_{0\text{-RSJ-}1.08}$. On the other hand, when the preloading level increased to 95%, the proposed compound technique was capable to restore 67% (44 kN) of the lost strength gain (66 kN) due to preloading. The ultimate capacity of beam $B_{3\text{-IRSJ-}1.08}$ was 346 kN, about 94% of that achieved by beam $B_{0\text{-IRSJ-}1.08}$. The obtained results proved that the epoxy injection was well done.

3.2. Deformation analysis

Fig. 10 shows the load–deflection (mid-span deflection) curves of the tested beams. In addition, column 9 of Table 4 summarizes the values of mid-span deflection at ultimate. Fig. 10a shows the load–deflection curves of group I as well as the unstrengthened beam. For the unstrengthened beam BC, the occurrence of the shear cracks was accompanied with a sudden reduction in the beam stiffness. Approximately 28% reduction in the post-cracking beam's stiffness was recorded (the stiffness is considered the slope of load–deflection curve [54]). In addition, reaching the ultimate capacity, the control beam failed suddenly and the maximum deflection at ultimate was 5.35 mm. On the other hand, for group I, all beams exhibited a similar portion of the load–deflection response until reaching the first shear-crack load. Once the first crack took-place, the effect of the strengthening system was obvious. Using the SHCC jacket was able to control the degradation in post-cracking stiffness of group I. Moreover, this degradation decreased with increasing the jacket's reinforcement ratio. For beams $B_{0\text{-SJ-}0}$, $B_{0\text{-RSJ-}0.65}$, $B_{0\text{-RSJ-}0.86}$ and $B_{0\text{-RSJ-}1.08}$ the loss in post-cracking stiffness were 26, 23, 22 and 20%, respectively. This may be due to the fibers bridging action. The fibers intersecting with the crack's surfaces can resist the crack widening, thus, reduced the stiffness degradation. Furthermore, for the strengthened beams, a distinguished post-peak behaviour was observed, as, the strengthened beams showed a gradual drop of the load form peak to the release load (i.e. more ductile failure). As listed in Table 4, the maximum ultimate deflections of beams $B_{0\text{-SJ-}0}$, $B_{0\text{-RSJ-}0.65}$, $B_{0\text{-RSJ-}0.86}$ and $B_{0\text{-RSJ-}1.08}$ were 8.21, 8.57, 8.87 and 9.31 mm, respectively (higher than that of the unstrengthened beam BC, which means a more detectable failure).

Beams $B_{1\text{-SJ-}1.08}$, $B_{2\text{-SJ-}1.08}$ and $B_{3\text{-SJ-}1.08}$ were preloaded by 75, 85 and 95% of the ultimate load, and then, repaired by SHCC jackets. The load–deflection curves of these beams along with beams $B_{0\text{-RSJ-}1.08}$ (strengthened without preloading) and BC (unstrengthened beam) is shown in Fig. 10b. Firstly, as shown in Fig. 10b, the application of the

Table 4
Summary of test results.

Group No.	Beam ID	P_u, kN	G, kN	$P_{cr\text{-}flex}$, kN	$P_{cr\text{-}sh}$, kN		$\Delta_{cr,\ sh}$, mm	Δ_u, mm	E, kN·mm
					BR	AR			
Control	BC	180	–	90	96	–	2.51	5.35	776
Group I	$B_{0\text{-SJ-}0}$	285	105	92	–	140	3.40	8.21	1097
	$B_{0\text{-RSJ-}0.65}$	318	138	90	–	141	3.10	8.57	1271
	$B_{0\text{-RSJ-}0.86}$	341	161	93	–	142	2.82	8.87	1401
	$B_{0\text{-RSJ-}1.08}$	368	188	91	–	142	2.61	9.31	1775
Group II	$B_{1\text{-RSJ-}1.08}$	340	162	90	98	135	4.01	12.60	1720
	$B_{2\text{-RSJ-}1.08}$	329	151	94	96	131	4.20	12.88	1700
	$B_{3\text{-RSJ-}1.08}$	302	124	93	95	122	4.61	13.92	1677
Group III	$B_{1\text{-IRSJ-}1.08}$	358	178	92	98	142	3.71	12.60	1762
	$B_{2\text{-IRSJ-}1.08}$	353	173	95	97	140	4.12	13.97	1748
	$B_{3\text{-IRSJ-}1.08}$	346	166	93	98	139	4.31	14.00	1698

P_u = ultimate load; G = strength gain; $P_{cr\text{-}sh}$ = shear first crack load; BR = before repairing; AR = after repairing; $P_{cr\text{-}flex}$ = flexure first crack load; $\Delta_{cr,\ sh}$ = deflection corresponding to first shear crack load after repairing; Δ_u = deflection corresponding to ultimate load; E = absorbed energy.

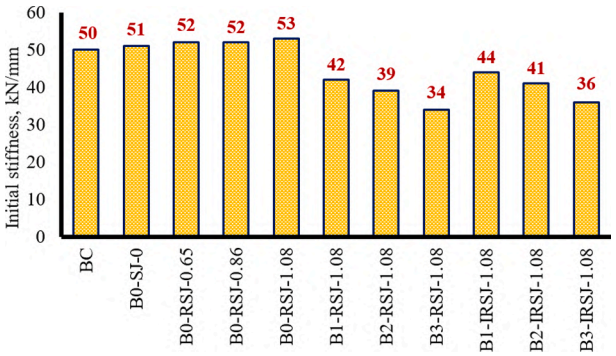


Fig. 11. Initial stiffness of the tested beams.

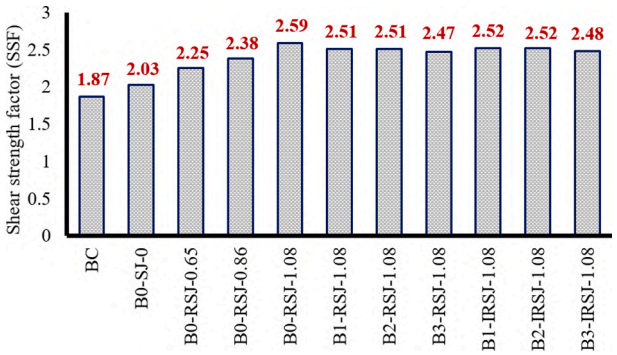


Fig. 12. Shear strength factors for the tested beams.

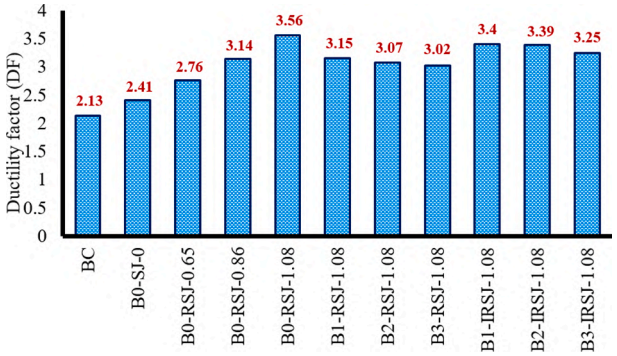


Fig. 13. Ductility factors for the tested beams.

reinforced SHCC jacket to the studied shear span cannot restore the uncracked stiffness to the pre-damaged beams. Furthermore, the beam's resistance to deformation decreased with increasing of the pre-loading degree. The elastic stiffness values of the tested beams are shown in Fig. 11. Beam $B_{3\text{-RSJ-}1.08}$ showed the least stiffness in comparison with the others. The recorded initial stiffness for $B_{3\text{-RSJ-}1.08}$ was about 68% of that of beam BC. This is mainly because the used repairing technique locally enhanced the stiffness of the repaired shear span, although the remaining cracked length that kept without strengthening is also affecting the beam's deflection. However, the strengthening technique did not enhance the preliminary stages of the load deflection response, at the post-peak stage, the response of the repaired beams was similar to that of beam $B_{0\text{-RSJ-}1.08}$ (strengthened without preloading), as the load decreased gradually without a sudden drop in load. At ultimate, the maximum deflections of beams $B_{1\text{-RSJ-}1.08}$, $B_{2\text{-RSJ-}1.08}$ and $B_{3\text{-RSJ-}1.08}$ were 12.60, 12.88 and 13.92 mm, respectively.

To evaluate the effect of cracks injection in conjunction with SHCC jacket, beams $B_{1\text{-SJ-}1.08}$, $B_{2\text{-SJ-}1.08}$ and $B_{3\text{-SJ-}1.08}$ were preloaded by 75, 85 and 95% of the ultimate load, and then, the formed cracks were injected with epoxy prior to the application of SHCC jacket. The load–deflection curves of the repaired beams of groups II and III as well as beams $B_{0\text{-RSJ-}1.08}$ (strengthened without preloading) and BC (unstrengthened beam) are shown in Fig. 10c. In general, as shown in Fig. 10c, the injected beams showed a slight improvement in the overall stiffness compared to the beams strengthened without injection, however, these stiffness are still less than that of the control beam (BC). It is worth mentioning that, the post-peak response of group III was quite similar to that obtained by groups I and II. At post ultimate stage, the beams exhibited a descending load pattern. At ultimate, the maximum deflections of beams $B_{1\text{-IRSJ-}1.08}$, $B_{2\text{-IRSJ-}1.08}$ and $B_{3\text{-IRSJ-}1.08}$ were 12.60, 13.97 and 14.00 mm, respectively.

3.3. Post-cracking shear strength and ductility

The analysis of the post-cracking shear strength of RC beams is important to predict the failure mode [37]. For the tested beams, the post-cracking shear strength was calculated using shear strength factor (SSF) proposed by previous researchers [60–62]. The SSF is defined as the ratio of the ultimate load (P_u) to the first shear crack load ($P_{cr,sh}$) as per Eq. (2).

$$SSF = \frac{P_u}{P_{cr,sh}} \tag{2}$$

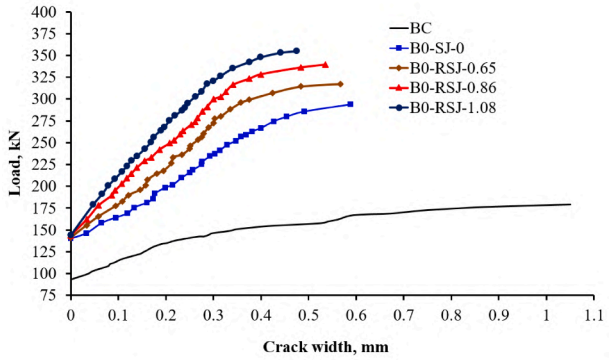
The ductility of the tested beams was expressed in terms of ductility factor (*DF*) as per Eq. (2) [62]. The ductility factor (*DF*) is defined as: the ratio of the deflection at ultimate load (Δ_u) to the deflection at first shear crack load ($\Delta_{cr,sh}$) [62]. For all beams, the DF values were calculated as per Eq. (3).

$$DF = \frac{\Delta_u}{\Delta_{cr,sh}} \tag{3}$$

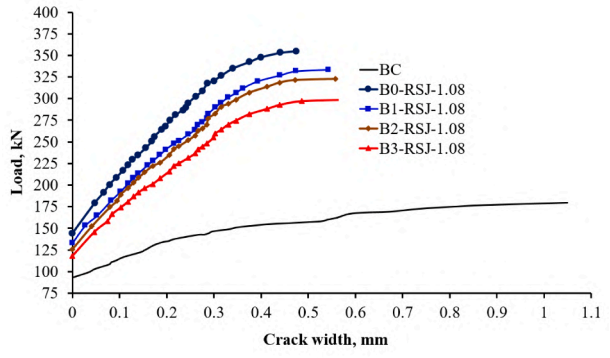
Figs. 12 and 13 show the calculated values of SSF and DF for all beams. Comparing the obtained results it was found that, the control beam BC showed the least values of both SSF (1.87) and DF (2.13). On the other hand, beam $B_{1\text{-RSJ-}1.08}$ showed the highest values of SSF (2.59) and DF (3.56). The strengthened beams showed a significant increase in ductility factors (SSF and DF) with increasing the jacket's reinforcement ratio. Increasing the reinforcement ratio form 0.65 to 1.08% was able to increase the SSF and DF by 15 and 28%, respectively, this observation is consistent with previous studies [63]. In contrast, the effect of pre-loading level showed to decrease slightly the ductility factors, however, the obtained values are still higher than that obtained for the control beam (BC). For instance, the DF of beam $B_{3\text{-RSJ-}1.08}$ was 3.02 vs. 2.13 for the control beam (BC). In addition, the use of epoxy injection was found to increase slightly the values of ductility factors. For instance, for beam $B_{1\text{-IRSJ-}1.08}$ the DF was 3.40 vs. 3.15 for beam $B_{1\text{-RSJ-}1.08}$. Even after comparing the calculated SSF and DF values, the used repairing techniques significantly enhanced the ductility of the repaired beams.

3.4. Absorbed energy

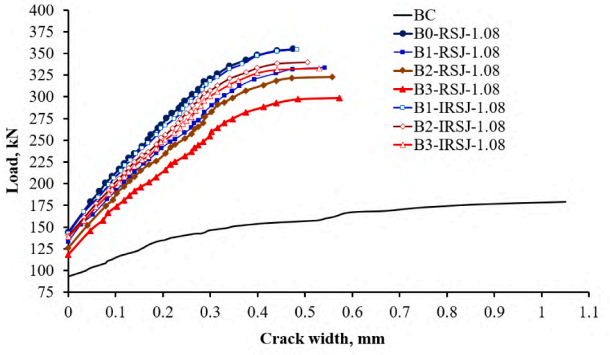
The values of the absorbed energy for all beams are reported in column 10 of Table 4. The absorbed energy was calculated by integrating the area under the load–deflection curve up to the post-peak load of 85% of the ultimate load (P_u) [61]. As reported in Table 4, the repaired beams showed significant enhancement in energy absorption capacities compared to the control beam (BC). Furthermore, this enhancement increased with the increase of jacket's reinforcement ratio. The value of energy absorption for beam $B_{0\text{-RSJ-}1.08}$ was 1775, which is more than twice the value of beam BC (776 kN·mm). This enhancement in absorbed energy is owing to the following two reasons: (1) the increase in ultimate capacity with the use of SHCC jacket; (2) the



(a) Curves of BC and group I



(b) Curves of BC, $B_{0\text{-}RSJ\text{-}0.72}$, group II



(c) Curves of BC, $B_{0\text{-}RSJ\text{-}0.72}$, group II and group III

Fig. 14. Load-crack width curves for the tested beams.

increase in ultimate deflection due to the enhanced ductility of the retrofitted beams.

For the preloaded beams, the value of the absorbed energy decreased with increasing of the preloading level. While, a slight enhancement was observed with the use of epoxy injection. For example, for beams $B_{1\text{-}RSJ\text{-}1.08}$, $B_{2\text{-}RSJ\text{-}1.08}$, and $B_{2\text{-}RSJ\text{-}1.08}$ the values of absorbed energy were 1720, 1700 and 1677 kN·mm, respectively. On the other hand, for beams $B_{1\text{-}IRSJ\text{-}1.08}$, $B_{2\text{-}IRSJ\text{-}1.08}$, and $B_{2\text{-}IRSJ\text{-}1.08}$ the values of absorbed energy were 1762, 1748, 1698 kN·mm, respectively. These values seem to be in accordance with the values of ductility factors. It can be concluded that, the proposed repairing technique significantly enhances the load carrying capacity as well as the ductility of shear-damaged beams.

3.5. Cracking behaviour

3.5.1. First shear-crack load

Columns 6 and 7 of Table 4 report the first shear-crack load before and after repairing, respectively. As reported in Table 4, the first-crack load of beam BC was 96 kN, which is similar to the pre-cracked beams of groups II and III before repairing (the cracking loads ranged between 95 and 98 kN). Whereas, for beams of group I, good results were obtained with the use of the SHCC jackets. The increase in shear-crack load ranged between 46% and 48% in comparison with the control beam (BC). This is to be expected, since, after the application of the SHCC jacket, the axial stiffness of the studied shear span increased. It worth mentioning that, the effect of jacket's reinforcement was insignificant, as, almost similar first-crack loads were recorded; 141, 142 and 142 kN for beams $B_{0\text{-}RSJ\text{-}0.65}$, $B_{0\text{-}RSJ\text{-}0.86}$ and $B_{0\text{-}RSJ\text{-}1.08}$, respectively.

Table 5
Crack width readings at different loads.

Group No.	Beam ID	$W_{k,max}$, mm (%)[a]			
		At 135[b] kN	At 153[c] kN	At 171[d] kN	At ultimate loads
Control	BC	0.20 (100%)	0.41 (100%)	0.73 (100%)	1.05 (100%)
Group I	$B_{0\text{-}SJ\text{-}0}$	–[e]	0.05 (12%)	0.12 (16%)	0.58 (55%)
	$B_{0\text{-}RSJ\text{-}0.65}$	–[e]	0.03 (7%)	0.09 (12%)	0.56 (64%)
	$B_{0\text{-}RSJ\text{-}0.86}$	–[e]	0.03 (7%)	0.05 (7%)	0.53 (50%)
	$B_{0\text{-}RSJ\text{-}1.08}$	–[e]	0.02 (5%)	0.04 (5%)	0.47 (45%)
Group II	$B_{1\text{-}RSJ\text{-}1.08}$	0.01 (5%)	0.03 (7%)	0.06 (8%)	0.54 (51%)
	$B_{2\text{-}RSJ\text{-}1.08}$	0.02 (10%)	0.04 (10%)	0.08 (11%)	0.55 (52%)
	$B_{3\text{-}RSJ\text{-}1.08}$	0.04 (20%)	0.06 (15%)	0.11 (15%)	0.57 (54%)
Group III	$B_{1\text{-}IRSJ\text{-}1.08}$	–[e]	0.02 (5%)	0.05 (6%)	0.47 (44%)
	$B_{2\text{-}IRSJ\text{-}1.08}$	–[e]	0.03 (7%)	0.06 (8%)	0.51 (48%)
	$B_{3\text{-}IRSJ\text{-}1.08}$	–[e]	0.03 (7%)	0.07 (9%)	0.52 (49%)

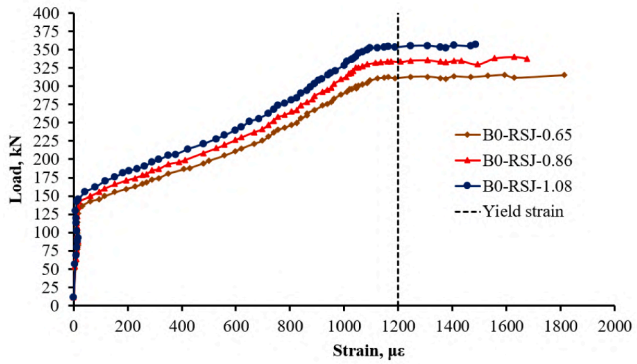
$W_{k,max}$ = maximum crack width; [a]ratio of crack width to that of beam BC = $\frac{crackwidth}{crackwidthofbeamBC} x100$; [b]the first preloading level; [c]the second preloading level; [d]the third preloading level; [e]the beam did not reach the cracking load.

For group II that were preloaded by 75, 85 and 95% of the ultimate load, then, these beams were repaired by SHCC jackets. Comparing the first-crack load results listed in Table 4, the increase of preload decreased the first-crack load. The first-crack loads of beams $B_{1\text{-}RSJ\text{-}1.08}$ (preloaded by 75%), $B_{2\text{-}RSJ\text{-}1.08}$ (preloaded by 85%) and $B_{3\text{-}RSJ\text{-}1.08}$ (preloaded by 95%) were 135, 131 and 122 kN, respectively (still higher than that of the same beam before repairing). This reduction correlates well with the modified compression field theory [64] which considered the aggregate interlocking as a primary shear-resisting component in the concrete beams, and the increase in preloading level decreased the aggregate interlocking [58].

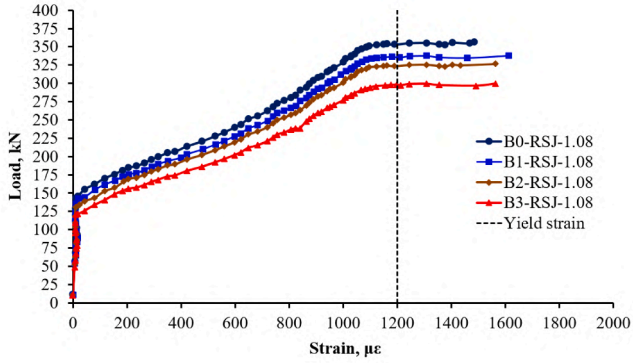
Regarding to the beams of group III, which were repaired by epoxy injection in conjunction with SHCC jackets. As listed in Table 4, injecting the shear cracks with epoxy prior to the application of the SHCC jackets enabled group III to record higher shear-crack loads compared to those of group II (strengthened without preloading). Beams $B_{1\text{-}IRSJ\text{-}1.08}$, $B_{2\text{-}IRSJ\text{-}1.08}$ and $B_{3\text{-}IRSJ\text{-}1.08}$ achieved first-crack loads of 142, 140 and 139 kN, respectively. This increase in first-crack resistance represents the impact of the used epoxy injection.

3.5.2. Crack width development

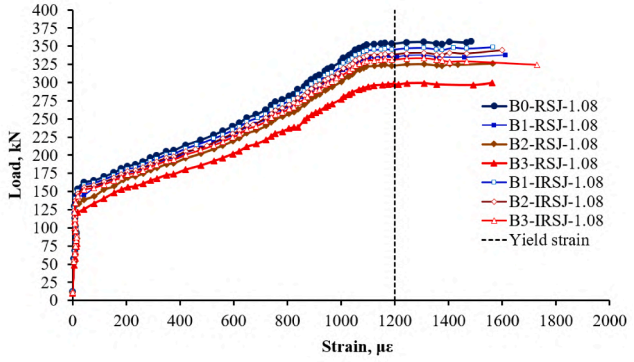
Fig. 14a to 14c show the load vs. shear-crack width curves of the tested beams. In addition, Table 5 summarizes the records of the maximum shear-crack widths at different loads of 135, 153, 171 kN and at ultimate load. As can be seen in Fig. 14a, once the control beam BC reached its cracking resistance (96 kN), a rapid increase in the crack width was observed and reached about 1.05 mm at ultimate. With regard to the strengthened beams of group I, the strain hardening phenomena and the fibers bridging action of SHCC resulted in fine



(a) Curves of group I



(b) Curves of $B_{0\text{-RSJ-0.72}}$, group II



(c) Curves of $B_{0\text{-RSJ-0.72}}$, group II and group III

Fig. 15. Load-strain curves for the intermediate-stirrup in SHCC jackets.

numerous cracks. For example, at a load of 171 kN, the crack width of beam $B_{0\text{-SJ-0}}$ was 0.12 mm vs. 0.73 mm for beam BC (i.e the crack width reduced to about 16% after using the SHCC jacket). Furthermore, the increase in jacket's reinforcement ratio played a key role in reducing the tensile stress on fibers, thus, more enhancement regarding the crack width measurements was achieved. As can be seen in Table 5, at a load of 171 kN, the crack-width of beam $B_{0\text{-RSJ-1.08}}$ was 0.04 mm, which represents only 5% of that of beam BC.

For the beams of group II that were preloaded by 75, 85 and 95% of the ultimate load, afterwards, these beams were repaired by SHCC jackets (1.08% reinforcement ratio). As depicted in Fig. 14b, the crack-arresting action of SHCC altered the cracking behaviour of the pre-cracked beams. At all loading levels, these beams showed less crack-width than that of the control beam. For example, as shown in Table 5, the severely pre-cracked beam $B_{3\text{-RSJ-1.08}}$ showed a decrease in crack width reached about 85% at load of 171 kN (the preloading of the same beam). It is worth mentioning that, the enhancement in crack-width measurements decreased with the increase of preloading level. At load of 171 kN, the crack widths of beams $B_{1\text{-RSJ-1.08}}$, $B_{2\text{-RSJ-1.08}}$ and $B_{3\text{-RSJ-1.08}}$ were 0.06, 0.08 and 0.11 mm, respectively.

Regarding to the beams of group III, the injection seems to be an effective technique for closing the cracks, which developed at the preliminary loading stage. As can be seen in Fig. 14c, the shear crack response of group III were almost similar to that of beam $B_{0\text{-RSJ-1.08}}$ (strengthened without preloading). As reported in Table 5, at load of 171 kN, the crack widths of beams $B_{1\text{-IRSJ-1.08}}$, $B_{2\text{-IRSJ-1.08}}$ and $B_{3\text{-IRSJ-1.08}}$ were 0.05, 0.06 and 0.07 mm, respectively, vs. 0.04 mm for beam $B_{0\text{-RSJ-1.08}}$.

3.6. Strain response

Fig. 15a–c show the shear load vs. the strain value of the intermediate steel stirrup in the SHCC jackets. Regarding the beams of group I, which were strengthened using SHCC jackets having three different reinforcement ratios, as expected, the stirrup strain decreased within the increase of jacket's reinforcement ratio. On the other hand, for group II, the stirrup strain increased within the increase of preloading level. In fact, increasing the pre-damage level reduced the shear resistance of concrete, then, the force transferred to the jacket was increased. The strain curves of groups II and III are plotted in Fig. 15c. Comparing the counterparts, at the same load level, the stirrup strain of the injected beam was less than that of the repaired without injection. This may be due to; the used epoxy injection infiltrated in to the cracks, and restored the cohesion between the cracked parts. Accordingly, after increasing the concrete resistance, the force transferred to the SHCC jacket was decreased.

4. Shear strength of SHCC-concrete beams

4.1. General

The ultimate shear capacity of the RC SHCC-jacketed beams can be determined by summation of the shear capacities of the following: concrete section, web reinforcement and gain of SHCC jacket, as given in Eq. (4).

$$V_u = V_c + V_s + V_{SHCC} \tag{4}$$

where V_u = ultimate shear capacity, V_c = shear capacity of concrete; Vs = shear capacity of web reinforcement; V_{SHCC} = shear capacity of SHCC.

4.2. Shear capacity according to japan society of civil engineers recommendations (JSCE)

JSCE [65] proposed the following equation (Eq. (5)) for estimating the shear capacity of concrete.

$$V_{cd} = \beta_d . \beta_p . f_{vcd} . b_w . d \tag{5}$$

where

$$f_{vcd} = 0.14 \sqrt[3]{f'_{cd}} \leq 0.5\text{MPa} \tag{6}$$

$$\beta_d = \sqrt[4]{\frac{1000}{d}} \leq 1.5 \tag{7}$$

$$\beta_p = \sqrt[3]{100 \rho_w} \leq 1.5 \tag{8}$$

where; V_{cd} = shear capacity of concrete; f'_{cd} = concrete compressive strength (MPa units).

On the other hand, according to JSCE [65] the shear capacity of the web reinforcement can be estimated as per the following Eq. (9).

$$V_s = \frac{A_w * f_{ys}}{S} d \tag{9}$$

Table 6
JSCE prediction models versus the experimental results.

	Beam ID	P_u, kN	Experimental			JSCE prediction			
			Vc + Vs, kN	V_{SHCC}, kN	V_{exp}, kN	Vc + Vs, kN	V_{SHCC}, kN	$V_{anal.}$, kN	V_{exp}/V_{analy}
Control	BC	180	90.0	–	90.0	58.9	–	58.9	1.53
Group I	$B_{0\text{-}SJ\text{-}0}$	285	90.0	52.5	142.5	58.9	52.8	111.7	1.27
	$B_{0\text{-}RSJ\text{-}0.65}$	318	106.5	52.5	159.0	75.2	52.8	128.0	1.24
	$B_{0\text{-}RSJ\text{-}0.86}$	341	118.0	52.5	170.5	80.6	52.8	133.4	1.28
	$B_{0\text{-}RSJ\text{-}1.08}$	368	131.5	52.5	184.0	86.0	52.8	138.8	1.32
Group II	$B_{1\text{-}RSJ\text{-}1.08}$	340	117.5	52.5	170.0	86.0	52.8	138.8	1.22
	$B_{2\text{-}RSJ\text{-}1.08}$	329	112.0	52.5	164.5	86.0	52.8	138.8	1.19
	$B_{3\text{-}RSJ\text{-}1.08}$	302	98.5	52.5	151.0	86.0	52.8	138.8	1.09
Group III	$B_{1\text{-}IRSJ\text{-}1.08}$	358	126.5	52.5	179.0	86.0	52.8	138.8	1.29
	$B_{2\text{-}IRSJ\text{-}1.08}$	353	124.0	52.5	176.5	86.0	52.8	138.8	1.27
	$B_{3\text{-}IRSJ\text{-}1.08}$	346	120.5	52.5	173.0	86.0	52.8	138.8	1.25
								Mean	**1.27**
								COV	**0.080**

P_u = total ultimate load; $V_{exp.}$ = experimental ultimate shear force = $0.5\,P_u$; V_c = concrete resistance; V_s = shear resistance of stirrups; V_{SHCC} = shear resistance of SHCC matric; $V_{anal.}$ = analytical shear force.

where; A_w = Area of web reinforcement; f_{ys} = yield strength of web reinforcement; S = Spacing of stirrups.

According to JSCE recommendations [65] the shear capacity of the SHCC matrix is the sum of the fibers bridging stress and the contact stress on the shear-crack surface. Accordingly, the shear capacity of the SHCC matrix can be calculated as per Eq. (10).

$$V_{SHCC} = 0.18 * \sqrt{f_c'} * t_{SHCC} * d_{SHCC} + \frac{f_{ty}}{tan\beta} * t_{SHCC} * Z \quad (10)$$

where; f_c' = SHCC compressive strength; t_{SHCC} = SHCC jacket thickness; d_{SHCC} = SHCC jacket depth; f_{ty} = first cracking strength of SHCC matrix; β = inclination angle of the shear-crack with respect to the beam axis (In this study the value of β angle is considered equals to 25° which represents the inclination of the line connecting the load with the support); $z = d_{SHCC}/1.15$.

4.3. Test results in comparison with JSCE code recommendations

The experimental and analytical results are presented in Table 6. As presented in Table 6, the prediction model of JSCE code gave good predictions to the contribution of the SHCC jacket to the shear capacity; the average value of the experimental to analytical was 0.99. However, JSCE code underestimated the total shear capacity of the strengthened/repaired beams with average safety margin of 27%. It is worth mentioning that, the pre-cracked beams of group II showed the least values of $V_{exp.}/V_{anal.}$ This is to be expected, as the preloading showed to decrease the aggregate interlocking of cracked concrete, subsequently, the experimental shear capacity was decreased.

5. Conclusion

Based on the experimental results and observations of this research; the following conclusions can be drawn:

- The use of SHCC jacket significantly increased the ultimate capacity of the tested beams. The improved degree of ultimate capacity of the jacketed beams increased with increasing the SHCC jacket's reinforcement ratio. Whereas, with the increase of preloading level, the shear strength gain of the repaired beams significantly decreased. The loss in strength gain reached about 34% with the highest preload level of 95% of the ultimate load. However, the use of epoxy injection prior to the application of the SHCC jacket showed its ability to restore a significant value of the lost strength gain. The percentage of this restored gain is dependent on the preload level, and reached about 67% with the highest preload level of 95% of the ultimate load.
- The application of SHCC jacket to cracked and uncracked beams showed a great improvement in the post-peak response. In comparison with the unstrengthened beam, the strengthened/repaired beams showed higher values of the ductility factors as well as the absorbed energy. This improvement increased with increasing the jacket's reinforcement ratio. However, using the proposed repairing technique with pre-cracked beams was not able to restore the initial stiffness of the uncracked beam. In addition, the use of epoxy injection made a slight increase in the initial stiffness of the repaired beams.
- The SHCC jacketed beams experienced a superior cracking performance in terms of load crack-width response and first shear-crack load as compared to the unstrengthened beam. The immense improvement in the cracking behaviour altered the cracking pattern of the preloaded beams after the application of the SHCC jacket. For all repaired beams, at the same load level, the measured crack width was less 20% of that measured for the unstrengthened beam.
- The prediction model of JSCE code gave good predictions to the contribution of the SHCC jacket to the shear capacity; the average ratio of experimental to theoretical was 0.99. However, JSCE code underestimated the total shear capacity of the strengthened/repaired beams with average safety margin of 27%.

CRediT authorship contribution statement

Ali Hassan: Writing - original draft, Writing - review & editing. **Ahmed T. Baraghith:** Conceptualization, Data curation. **Ahmed M. Atta:** Conceptualization, Data curation. **Tarek F. El-Shafiey:** Supervision.

Declaration of Competing Interest

The authors declare that they have no known competing financial interests or personal relationships that could have appeared to influence the work reported in this paper.

References

[1] Hawileh R, Rasheed H, Abdalla J, Al-Tamimi A. Behavior of reinforced concrete beams strengthened with externally bonded hybrid fiber reinforced polymer systems. Mater Des 2014;53:972–82. https://doi.org/10.1016/j.matdes.2013.07.087.
[2] Hawileh RA, El-Maaddawy TA, Naser Z. Nonlinear finite element modeling of concrete deep beams with openings strengthened with externally-bonded composites. Mater Des 2012;42:378–87.
[3] Rasheed H, Larson K, Peterman R. Analysis and design procedure for FRP strengthened prestressed concrete T-Girders considering strength and fatigue. J Compos Constr ASCE 2006;10(5):419–32.

[4] Hassan T, Rizkalla S. Investigation of bond in concrete structures strengthened with near surface mounted carbon fiber reinforced polymer strips. J Compos Constr 2003;7(3):248–57. https://doi.org/10.1061/(ASCE)1090-0268(2003)7:3(248).

[5] Pham T, Hao H. Behavior of fiber-reinforced polymer-strengthened reinforced concrete beams under static and impact loads. Int J Protect Struct 2017;8. https://doi.org/10.1177/2041419616658730.

[6] Hawileh R, Rasheed H, Abdalla A, Tamimi A. Behavior of reinforced concrete beams strengthened with externally bonded hybrid fiber reinforced polymer systems. J Mater Des 2014;53:972–82.

[7] Al-Amery R, Al-Mehaidi R. Coupled flexural-shear retrofitting of RC beams using CFRP straps. Compos. Struct. 2006;75:457–64.

[8] Abu-Obaida A, El-Maaddawy T, El-Ariss B. Numerical simulation of double-sided concrete corbels internally-reinforced with GFRP bars. Compos Part C 2020;100040. https://doi.org/10.1016/j.jcomc.2020.100040.

[9] Meier U. Strengthening of structures using carbon fibre/epoxy composites. Constr Build Mater 1995;6:341–51.

[10] Hawileh R, Nawaz W, Abdalla A, Saqan I. Effect of flexural CFRP sheets on shear resistance of reinforced concrete beams. Compos Struct 2015;122:468–76.

[11] Hussein M, Afefy HM, Khalil AA. Innovative repair technique for RC beams predamaged in shear. J Compos Constr 2013;17.

[12] Gao WY, Hu KX, Dai JG, Dong K, Yu KQ, Fang LJ. Repair of fire-damaged RC slabs with basalt fabric-reinforced shotcrete. Constr Build Mater 2018;185:79–92.

[13] Ding Z, Xu MR, Dai JG, Dong BQ, Zhang MJ, Hong SX, et al. Strengthening concrete using phosphate cement-based fiber-reinforced inorganic composites for improved fire resistance. Constr Build Mater 2019;212:755–64.

[14] Azam R, Soudki K. FRCM strengthening of shear-critical RC beams. J Compos Constr 2014;18(5):04014012.

[15] Wakjira TG. Ebead U.A shear design model for RC beams strengthened with fabric reinforced cementitious matrix. Eng Struct 2019;200(109698). https://doi.org/10.1016/j.engstruct.2019.109698.

[16] Jiang CJ, Lu ZD, Li LZ. Shear performance of fire-damaged reinforced concrete beams repaired by a bolted side-plating technique. J Struct Eng – ASCE 2017;143(5):04017007.

[17] Li LZ, Wu ZL, Yu JT, Wang X, Zhang JX, Lu ZD. Numerical simulation of the shear. Capacity of bolted side-plated RC beams. Eng Struct 2018;171:373–84.

[18] Mohamed M, Oehlers D, Bradford M. Shear peeling of steel plates adhesively bonded to the sides of reinforced concrete beams. Proc Inst Civil Eng – Struct Build 2000;3(140):249–59.

[19] Oehlers DJ, Liu IST, Seracino R. Shear deformation debonding of adhesively bonded plates. Proc Inst Civil Eng – Struct Build 2005;158(1):77–84. https://doi.org/10.1680/stbu.2005.158.1.77.

[20] Li LZ, Lo SH, Su RKL. Experimental study of moderately reinforced concrete beams strengthened with bolted-side steel plates. Adv Struct Eng 2013;16(3):499–516.

[21] Lo SH, Li LZ, Su RKL. Optimization of partial interaction in bolted side-plated reinforced concrete beams. Comput Struct 2014;131(7):70–80.

[22] Li Ling-Zhi, Chang-Jiu J, Kai-Leung S, Sai-Huen L. Design of bolted side plated reinforced-concrete beams with partial interaction. Proc Inst Civil Eng – Struct Build 2016;169(2):81–95. https://doi.org/10.1680/jstbu.15.00037.

[23] Li LZ, Jiang CJ, Su RKL, Lo SH. A piecewise linear transverse shear transfer model for bolted side-plated beams. Struct Eng Mech 2017;62(4):443–53.

[24] Su RKL, Li LZ, Lo SH. Shear transfer in bolted side-plated reinforced concrete beams. Eng Struct 2013;56(11):1372–83.

[25] Su RKL, Li LZ, Lo SH. Longitudinal partial interaction in bolted side-plated reinforced concrete beams. Adv Struct Eng 2014;17(7):921–36.

[26] Li VC, Leung CKY. Steady state and mutiple cracking of short random fiber composites. ASCE J Eng Mech 1992;118(11):2246–64.

[27] Mündecke E, Mechtcherine V. Tensile behaviour of strain-hardening cement-based composites (SHCC) with steel reinforcing bars. Cem Concr Compos 2020;105:103423.

[28] Li J, Weng J, Yang E. Stochastic model of tensile behavior of strain-hardening cementitious composites (SHCCs). Cem Concr Res 2019;124:105856.

[29] Li VC. On engineered cementitiouscomposities (ECC), a review of the material and its applications. J Adv Concr Technol 2003;1:215–30.

[30] Fukuyama H, Matsuzaki Y, Nakano K, Sato Y. Structural performance of beam elements with PVA-ECC. In: Reinhardt Naaman A, editor. Proc of high performance fiber reinforced cement composites 3 (HPFRCC 3). Chapman & Hull; 1999. p. 531–42.

[31] Kanda T, Li VC. New micromechanics design theory for pseudo strain-hardening cementitious composites. ASCE J Eng Mech 1999;125(4):373–81.

[32] Li VC. From micromechanics to structural engineering – the design of cementitious composites for civil engineering applications. J Struct Mech Earthq Eng 1993;10:37–48.

[33] Li VC. Engineered cementitious composites (ECC) – tailored composites through micromechanical modeling. In: Fiber reinforced concrete: present and the future; 1998. p. 64–97.

[34] Yu J, Leung CKY. Strength improvement of strain-hardening cementitious composites with UltrahighVolume fly ash. J Mater Civ Eng 2017;29:05017003.

[35] Ueda T, Dai J. Interface bond between FRP sheets and concrete substrates: properties, numerical modeling and roles in member behavior. Prog Struct Eng Mater 2005;7:27–43. https://doi.org/10.1002/pse.187.

[36] Xue H, Deng Z. Experimental study of engineering cementitious composites. J Southeast Univ 2010;40:20–7.

[37] Wang N. Experimental research on bonding mechanical performance between ultra high toughness cementitious composites (UHTCC) and existing concrete. Dalian: Dalian University of Technology; 2010.

[38] Slowik V, Luković M, Wagner C, et al. Behaviour of bonded SHCC overlay systems. In: A framework for durability design with strainhardening cement-based composites (SHCC), RILEM; 2017. p. 125–46. ISBN 978-94-024-1012-9.

[39] Kim YY, Fischer G, Lim YM, Li VC. Mechanical performance of sprayed engineered cementitious composite using wet-mix shotcreting process for repair applications. ACI Mater J 2004;101(1):42–9.

[40] Afefy HM, Kassem NM, Hussein M. Enhancement of flexural behavior of CFRP strengthened reinforced concrete beams using engineered cementitious composites transition layer. Struct Infrastruct Eng 2015;11(8):1042–53.

[41] Kassem M, El-Shafeiy T, Hussein M, Afefy H, Hassan A. Shear behaviour of SHCC dry joints in precast construction international conference on advances in structural and geotechnical engineering, ICASGE'17, Hurghada, Egypt; 27–30 March 2017.

[42] Afefy HM, Baraghith AT, Hassan A, Abuzaid MK. Strengthening of shear-deficient RC beams using near surface embedded precast cement-based composite plates (PCBCPs). Eng Struct 2021;214:112765. https://doi.org/10.1016/j.engstruct.2021.112765.

[43] Fischer G, Li VC. Deformation behavior of fiber-reinforced polymer reinforced engineered cementitious composite (ECC) flexural members under reversed cyclic loading conditions. ACI Struct J 2003;100:25–35.

[44] Li VC, Li M. Durability performance of ductile concrete structures. In: Proceedings of the 8th international conference on creep, shrinkage and durability of concrete and concrete structures, Ise-Shima, Japan; 2008. p. 761–8.

[45] Sahmaran M, Li M, Li VC. Transport properties of engineered cementitious composites under chloride exposure. ACI Mater J 2007;104:604–11.

[46] Li M, Li VC. Cracking and healing of engineered cementitious composites under chloride environment. ACI Mater J 2011;108:333–40.

[47] Kim SW, Park WS, Jang YI, Feo L, Yun HD. Crack damage mitigation and shear behavior of shear-dominant reinforced concrete beams repaired with strain-hardening cement-based composite. Compos Part B Eng 2015;79:6–19.

[48] Wang G, Yang C, Pan Y, Zhu F, Jin K, Li K, et al. Shear behaviors of RC beams externally strengthened with engineered cementitious composite layers. Materials 2019;12:2163. https://doi.org/10.3390/ma12132163.

[49] Baghi H, Barros JAO, Rezazadeh M. Shear strengthening of damaged reinforced concrete beams with Hybrid Composite Plates. Compos Struct 2017;178:353–71. https://doi.org/10.1016/j.compstruct.2017.07.039.

[50] Zheng YZ, Wang WW, Mosalam KM, Fang Q, Chen L, Zhu ZF. Experimental investigation and numerical analysis of RC beams shear strengthened with FRP/ECC composite layer. Compos Struct 2020;246:112436. https://doi.org/10.1016/j.compstruct.2020.112436.

[51] Yang X, Gao WY, Dai JG, Lu ZD. Shear strengthening of RC beams with FRP grid-reinforced ECC matrix. Compos Struct 2020;241:112120. https://doi.org/10.1016/j.compstruct.2020.112120.

[52] Shang Xy Yu, Jt Li Lz, Lu Zd. Shear strengthening of fire damaged RC beams with stirrup reinforced engineered cementitious composites. Eng Struct 2020;210:110263. https://doi.org/10.1016/j.engstruct.2020.110263.

[53] Hassan A, Atta AM, El-Shafiey TF. Restoration of the shear capacity for RC beams with web openings using precast SHCC plates. Structures 2020;25:603–12. https://doi.org/10.1016/j.istruc.2020.03.046.

[54] Collins MP, Mitchell D. Prestressed concrete structures. Englewood Cliffs, NJ: Prentice-Hall; 1997.

[55] Witchukreangkrai E, Mutsuyoshi H, Takagi M, De Silva S. Evaluation of shear crack width in partially prestressed concrete members. Proc JCI 2006;28(2):823–8.

[56] Rizkalla SH, Hwang LS, El Shahawai M. Transverse reinforcement effect on cracking behavior of RC members. Canadian J Civil Eng 1983;10(4):566–81.

[57] Hassan HM. Shear cracking behavior and shear resisting mechanism of reinforced concrete beams with web reinforcement. PhD. Thesis. Japan: University of Tokyo; 1987.

[58] Kunieda M, Hussein M, Ueda N, Nakamura H. Enhancement of crack distribution of UHP-SHCC under axial tension using steel reinforcement. J Adv Concr Technol 2010;8:49–57.

[59] Sherwood EG, Bentz EC, Collins MP. Effect of aggregate size on beam-shear strength of thick slabs. ACI Struct J 2007;104(2):180–90.

[60] Hossain KMA, Hasib S, Manzur T. Shear behavior of novel hybrid composite beams made of self-consolidating concrete and engineered cementitious composites. Eng Struct 2020;202:109856. https://doi.org/10.1016/j.engstruct.2019.109856.

[61] Hassan AAA, Hossain KMA, Lachemi M. Strength, cracking and deflection performance of large-scale self-consolidating concrete beams subjected to shear failure. Eng Struct 2010;32(5):1262–71.

[62] Mazzotti C, Savoia M. Long-term deflection of reinforced self-consolidating concrete beams. ACI Struct J 2009;106(6):772–81.

[63] Shin SK, Kim JJH, Lim YM. Investigation of the strengthening effect of DFRCC applied to plain concrete beams. Cem Concr Compos 2007;29:465–73.

[64] Vecchio FJ, Collins MP. The modified compression-field theory for reinforced concrete elements subjected to shear. J Struct 1986;83(2):219–31.

[65] Japan Society of Civil Engineers. Recommendations for design and construction of high performance fiber reinforced cement composite with multiple fine cracks (HPFRCC), Concrete engineering series 82; 2008.